Low-Interference Sensing Electronics For High-Resolution Error-Correcting Biomechanical Ground Reaction Sensor Cluster

Michael A. Suster, Carlos Mastrangelo and Darrin J. Young
Department of Electrical and Computer Engineering
The University of Utah
Salt Lake City, Utah, USA
darrin.young@utah.edu

Abstract— **This paper presents a low-interference and low – power sensing electronics design for a high-resolution error-correcting biomechanical ground reaction sensor cluster (GRSC) developed for improving inertial measurement unit (IMU) positioning resolution and accuracy. The GRSC is composed of 13 x 13 sensing nodes, which can measure dynamic ground forces, shear strains, and sole deformation associated with a ground locomotion gait. The integrated sensing electronics consist of a front-end multiplexer that can sequentially connect individual sensing nodes in a GRSC to a capacitance-to-voltage converter followed by an ADC, digital control unit, and driving circuitry to interrogate the GRSC. The sensing electronics are designed in a 0.15 µm CMOS process and occupy an area of approximately 3 mm^2 with an expected resolution of 10-bits and 14-bits for the z-axis pressure sensing and the x and y-axes shear strain sensing, respectively, while dissipating a DC power less than 2 mW from a 3V supply.**

I. INTRODUCTION

It is highly desirable to track a person's physical location in a GPS-denied environment, for example a fire fighter in a rescue mission, a traveler in a remote area, or a soldier in battlefield. Commercially available inertial measurement units (IMUs) have been explored for such applications. However, these IMUs exhibit an excessive output drift over time, thus unsuitable for determining an accurate position. It was recently demonstrated that a personal navigation system can be achieved by employing a high-resolution-gait-corrected IMU [1]. The system combines a commercial off-the-shelf (COTS) IMU with a thin and flexible error-correcting biomechanical ground reaction sensor cluster (GRSC). The IMU and GRSC are placed within the heel and at the sole of a personnel boot, as shown in Figure 1, and wirelessly connected to a handheld unit, which can process inertial and GRSC data in real time. In this approach the IMU can measure inertial displacements while the biomechanical GRSC can independently measure dynamic ground forces, shear strains, and sole deformation associated with a ground locomotion gait. In human bipedal locomotion, the walking mode or gait consists of two separate phases as depicted in Figure 2 [2]. In the swing phase, the leg is off the ground. This period extends from the instant the toe leaves the ground until the heel strikes. In the stance phase, the foot heel first contacts the ground, then it rolls until the midstance is reached, resulting in pivoting of the leg on the ankle and corresponding forward motion of the body. Beyond midstance, detachment of the foot takes place through a gradual rolling. It is evident that only during a fraction of the midstance the velocity of the heel is exactly zero [3]. Pressure sensors array can be used to detect pressure contours that are generated by the heel if the array is placed between the heel of the shoe and the shoe insole. The pressure contours movement as depicted in Figure 3 can calculate periods of zero velocity accurately during the stance phase in a human bipedal locomotion. These zero velocity points in turn can provide discrete zero velocity corrections to the IMU, thus dramatically increasing the positioning accuracy.

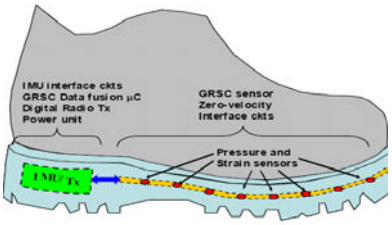

Figure 1. IMU and GRSC embedded personal boot.

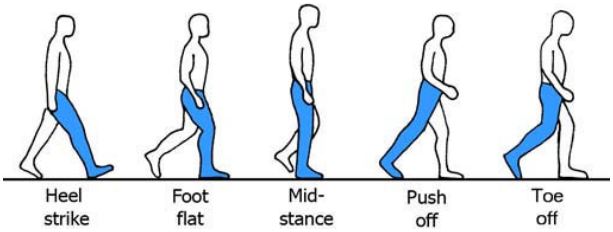

Figure 2. Stance phase in human bipedal locomotion.

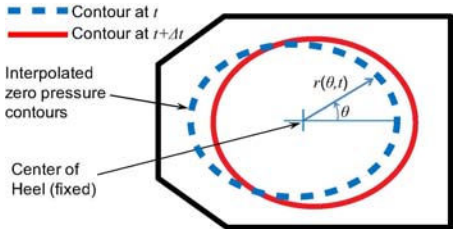

Figure 3. Pressure contours movement during stance phase.

Step-corrected (also known as dead reckoning) IMU and GPS navigation systems have been in existence [4-10]. However, these systems detect the step impact shock by employing accelerometers placed away from the ground. This approximate detection technique typically results in a large positioning error, around 1-2% of the distance traveled. In the proposed architecture, a data-rich high-resolution GRSC is placed very close to the point of heel to ground contact, thus providing detailed contact information to an IMU located in a close proximity to the GRSC. This extra information and the close mechanical (near rigid) relation between the velocity at the GRSC and IMU location are the key to achieve a high-accuracy positioning performance [11]. To verify the concept of employing pressure sensors array to detect zero velocities of the heel, which in turn update the IMU for improving positioning accuracy, a prototype boot incorporating a commercial insole-shaped pressure sensor array (Novel Pedar Pressure Sensor System) was built with an IMU mounted externally as shown in Figure 4; note that an optical marker tool frame was attached for velocity measurement as a reference.

Figure 4. Boot with pressure sensors array inserted in the insole and IMU externally mounted.

The pressure sensors array consists of 99 sensing elements, where 54 elements are located in the heel portion. Figure 5 presents the measure pressure contours super-imposed on the heel portion of the pressure sensor insole.

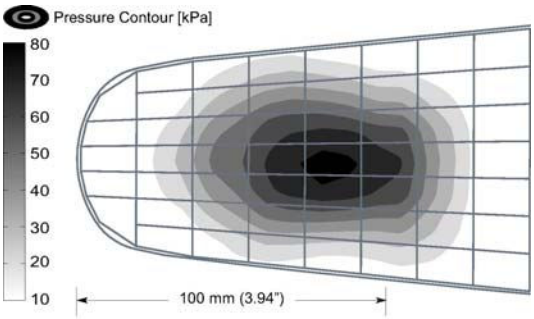

Figure 5. Pressure contours super-imposed on the heel portion of the pressure sensor insole.

Furthermore, a loop-closing ½ hour walk test was performed by using the prototypte boot with the nessary signal conditioning and processing algorithms [1]. The field test demonstrated a position error less than 4 meters. Figure 6 shows the walking conture in the field. A 5-minute walk around an 11.7m/edge squre (indicated by blue color) was first carried out for calibration purpose [1], followed by a ½ hour random walk with paths shown for illustrative purpose.

Figure 6. Field walking test contours.

To maintain the same positioning accuracy for an extended walking time, for example a number of hours for demanding applications, a GRSC with an increased density is required. More data points available from a high density array are expected to detect much smaller changes during the stationary contact of the heel, thus significantly reducing errors in the zero-velocity calculation during the stance phase. As the GRSC sensing resolution and accuracy increase, low-noise and low-interference sensing electronics become highly critical to accurately capture real-time dynamic response from a ground locomotion gait. A careful electronic system design is crucial to minimize environment noise and interference coupling due to the heel dynamic movement.

II. High Density Capacitive Pressure Sensors Array

A high density capacitive pressure sensors array consisting of 13 x 13 individual sensing nodes is designed and fabricated by employing flexible PDMS and gold layers for improving positioning accuracy. Figure 7 shows a schematic of such a design, where each sensing node can be accessed by the corresponding row and column connections. For navigation, pressure sensing along the vertical axis (z-axis) alone is insufficient as the GRSC must be capable of detecting shear force for determining slippage and shoe rotation estimation. Therefore, a combined capacitive pressure and shear strain sensing scheme, consisting of a quad-cell sensing capacitors arrangement that is sensitive to both normal pressure and shear strain, is incorporated inside each sensing node as depicted in Figure 8. Each sensing node contains two circular sensing units designed for z-axis pressure as well as differential x and y-axes shear strain sensing. Z-axis pressure measurements are achieved through

the deformation of the soft-polymer substrate. Shear strain along x and y-axes are detected by the sensing capacitors overlapping area change in a differential manner.

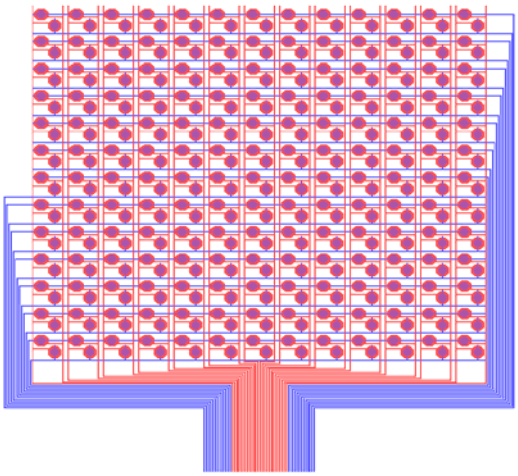

Figure 7. 13 x 13 capacitive pressure sensors array.

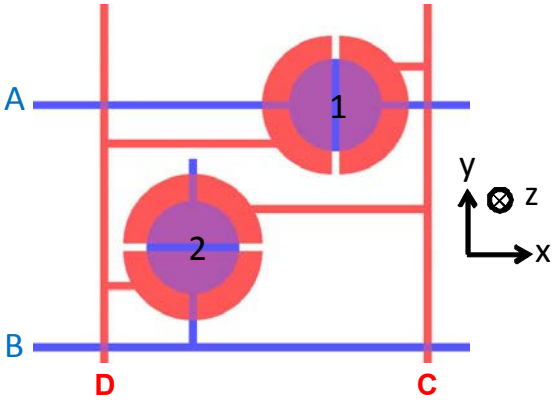

Figure 8. GRSC sensing node for pressure and shear strain sensing.

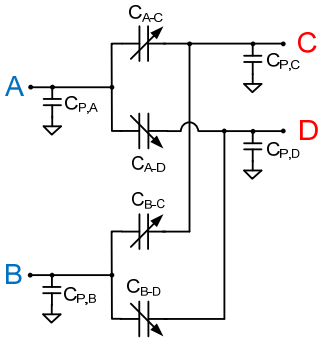

Figure 9. GRSC sensing node electrical model.

Each sensing unit exhibits a diameter of 1.2 mm with a PDMS thickness on the order of 15 µm, thus achieving a nominal capacitance of approximately 1 pF for each side of the differential capacitor with a pressure sensitivity around 1.6 fF/kPa. Figure 9 presents the corresponding electrical model of each capacitive sensing node. The pitch size between two adjacent sensing nodes is approximately 5 mm. This pitch size is chosen to achieve an expected velocity sensing resolution of 10 µm/sec, which is critical for enhancing the IMU positioning accuracy.

III. Low-Interference Sensing Electronics For Capacitive Pressure Sensors Array

Figure 10 presents the interface sensing electronic system design architecture, consisting of a front-end multiplexer that can sequentially connect 169 individual sensing nodes in a 13 x 13 GRSC to a capacitance-to-voltage (C/V) converter followed by a 12-bit ADC, digital control unit, and driving circuitry to interrogate the GRSC.

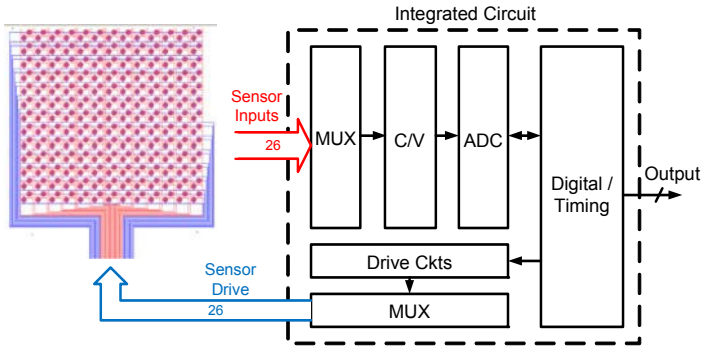

Figure 10. GRSC interface electronic system design architecture.

Each GRSC sensing node is made of two circular PDMS-based capacitive sensing units, as shown in Figure 8, exhibiting a nominal capacitance of 1pF, and a maximum capacitance change of 10% along the z-axis as well as the x and y-axes. The capacitive sensing units can be dynamically reconfigured by switches to achieve differential shear strain sensing (x and y-axes) and single-ended z-axis pressure sensing as modeled in Figure 9. The capacitive sensors are further interfaced with a charge amplifier as shown in Figure 11. Different switching schemes are designed for single-ended pressure sensing and differential shear strain sensing.

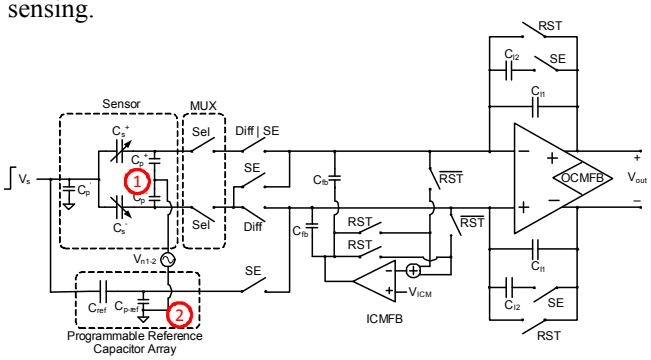

Figure 11. Charge amplifier for GRSC interface.

Input common-mode feedback circuit is incorporated to ensure the electronic sensing operation is immune to input

parasitic capacitance (mainly composed of capacitances from un-selected sensing nodes) and its mismatch [12]. The single-ended z-axis pressure sensing calls for a programmable reference capacitor array to ensure a close match with the sensor capacitance value, thus suppressing amplifier output offset voltage. In the proposed application, the PDMS-based GRSC is fabricated on a different substrate and is connected to the interface ASIC via an electrical connector. Therefore, an interference signal, $V_{n1\text{-}2}$, can be developed between the ground nodes of GRSC and ASIC labeled as node 1 and node 2 in Figure11. This ground interference will be amplified at the charge amplifier output, limiting the sensing resolution. The following expressions show the interference-signal transfer function for the single-ended z-axis pressure sensing channel and differential x and y-axes shear strain sensing channels, where C_p^+ and C_p^- are the parasitic capacitances associated with the selected sensors.

$$V_{on,se} = \frac{C_p^{+} + C_p^{-}}{C_{I1} + C_{I2}} V_{n1-2} \text{ and } V_{on,diff} = \frac{C_p^{+} - C_p^{-}}{C_{I1}} V_{n1-2}$$

It is evident that (1) the pressure sensing channel performance can be improved by reducing the number of sensing units attached to each GRSC row or column; hence the parasitic capacitances, however at an penalty of increased interconnect complexity, and (2) the shear strain sensing channel performance can be enhanced by matching the parasitic capacitances. A parasitic-matched GRSC sensing unit layout is, therefore, proposed in Figure 12 to minimize the interference effect.

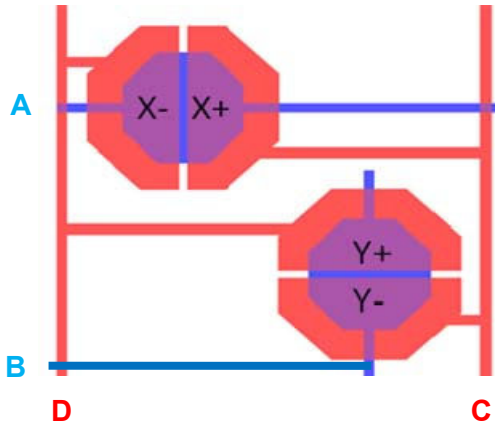

Figure 12. Parasitic-matched GSRC sensing unit layout.

Simulation reveals that with such a design a ground interference signal with a typical amplitude of 10μV peak-to-peak would result in a sensing resolution of 14-bits for the x and y-axes shear strain sensing channel and 10-bits for the z-axis pressure channel with an expected improvement by reducing the number of sensing units attached to each GRSC column but with an expense of increased interconnect complexity. This consideration and trade-off are critical for future higher density array design with an expectation to further improve IMU positioning accuracy. To meet the current resolution requirement of 12-bits, the electronics are designed with 2mW power dissipation from a 3V supply in a 0.15 μm CMOS process.

IV. Conclusion

High resolution GRSC based on high density capacitive sensors array is expected to significantly improve the IMU positioning accuracy for personal navigation application. Parasitic-matched GSRC sensing unit design is critical to prevent ground interference signal from degrading the overall system performance. Trade-off between system accuracy and interconnect complexity is an important consideration for achieving potential high-performance systems.

Acknowledgment

This work was supported by the U.S. Defense Advanced Research Projects Agency.

References

[1] O. Bebek, M. A. Suster, S. Rajgopal, M. J. Fu, X. Huang, M. C. Cavusoglu, D. J. Young, M. Mehregany, A. J. van den Bogert, and C. H. Mastrangelo, "Personal Navigation via High-Resolution-Gai-Corrected Inertial Measurement Units," to appear in *the IEEE Transactions on Instrumentation and Measurement*, 2010.

[2] M. Trew and T. Everett, *Human movement: an introductory text*, 4th edition, Elsevier Health Sciences, 2001.

[3] H. Lanshammar and L. Strandberg, "Horizontal floor reaction forces and heel movements during the initial stance phase," *Biomechanics VIII-B*, pp. 1123–1128, 1982.

[4] J. Kim, J.-G. Lee, G.-I. Jee, and T. K. Sung, "Compensation of gyroscope errors and gps/dr integration," in *Proc. IEEE Position Location and Navigation Symposium*, April 1996, pp. 464–470.

[5] W.-W. Kao, "Integration of gps and dead reckoning navigation systems," in *Proc. IEEE Vehicle Navigation and Information Systems Conference*, vol. 2, October 1991, pp. 635–643.

[6] E. S. Sazonov, T. Bunpus, S. Zeigler, and S. Marocco, "Classification of plantar pressure and heel acceleration patterns using neural networks," in *Proc. IEEE Neural Networks Conference*, vol. 5, July-August 2005, pp. 3007–3010.

[7] C. Randell, C. Djiallis, and H. Muller, "Personal position measurement using dead reckoning," in *Proc. IEEE International Symposium on Wearable Computers*, October 2005, pp. 166–173.

[8] L. Fang, P. J. Antsaklis, L. Montestruque, M. B. McMickell, M. Lemmon, Y. Sun, H. Fang, I. Koutroulis, M. Haenggi, M. Xie, and X. Xie, "Design of a wireless assisted pedestrian dead reckoning system - the NavMote experience," *IEEE Transactions on Instrumentation and Measurement*, vol. 54, no. 6, pp. 2342–2358, December 2005.

[9] S. Godha and G. Lachapelle, "Foot mounted inertial system for pedestrian navigation," *Measurement Science and Technology*, vol. 19, pp. 1–9, 2008.

[10] J. Borenstein, L. Ojeda, and S. Kwanmuang, "Heuristic reduction of gyro drift for personnel tracking systems," *The Journal of Navigation*, vol. 62, no. 1, pp. 41–58, January 2009.

[11] J. Cheung, M. Zhang, A. Leung, and Y. Fan, "Three-dimensional finite element analysis of the foot during standing-a material sensitivity study," *Journal of Biomechanics*, vol. 38, pp. 1045–1054, 2005.

[12] P. Cong, N. Chaimanonart, W. H. Ko, and D. J. Young, "A Wireless and Batteryless 10-bit Implantable Blood Pressure Sensing Microsystem with Adaptive RF Powering for Real-time Genetically Engineered Mice Monitoring," *IEEE Journal of Solid-State Circuits,* Vol. 44, No, 12, pp. 3631-3644 (Special Issue), December 2009.